

Efficient Spectral Imaging based on Imaging Systems with Scene Adaptation Using Tunable Color Pixels

Andy L. Lin, Francisco Imai; Canon USA R&D Center; San Jose, CA

Abstract

Conventional spectral imaging systems use a set of pre-determined filters to capture multi-band images. Liquid crystal tunable filters (LCTF) and active illumination allow reconfiguration of spectral sensitivities but these techniques have shortcomings such as latency due to multiple captures and the fact that the same filtering or illumination is applied to the whole frame of the image. There are emerging device technologies that allow independent adjustment of the filtering for each region or even at a pixel level of the imaging frame. The operation of such imaging systems is controlled by adapting to the scene based on scene analysis. Experiments were run by simulating a spectral imaging system which adjusts pixel sensitivities based on color information from the scene. As a result this new system exhibits superior performance compared to traditional spectral imaging systems in terms of color accuracy and imaging capture efficiency.

Introduction

Traditionally, spectral imaging has relied on the use of pre-determined set of filters that are mechanically or electronically adjusted to capture image bands with different spectral properties [1]. Spectral imaging has been confined to some niche high-end applications such as remote sensing [2] and artwork analysis and archiving [3]. The reason for not having consumer level spectral imaging products yet are due to several factors such as cost, bulkiness of the imaging system and lack of a compelling application. Some of the shortcomings of conventional spectral imaging systems are the need to increase the number of captured signals to increase spectral resolution. Moreover, spectral imaging systems are inherently by design very inefficient not just because of the tremendous redundancy in spectral information, but also because spectral imaging systems typically capture pre-determined channels regardless if there are meaningful information in the captured band.

Spectral imaging is also conceptually a sub-category of computational imaging since it extends the capabilities of digital imaging by encoding and computing wavelength of light instead of trichromatic signals. However, spectral imaging has not exploited exhaustively the property of imaging capture re-configurability that is typical in computational imaging systems. One reconfigurable system is the Agile Spectrum Imaging [4] that is based on an adjustable computer-controlled optical system using a diffraction grating to disperse rays into different colors combined with an electronically controlled mask in the optical path to control spectrum. Another spectral imaging with reconfigurable approach is the spectral vision system that uses an optical set-up with a liquid-crystal spatial light modulator to implement color filters [5]. Such implementations show the possibilities of computational spectral imaging.

Tunable Imaging Sensors

It is possible to make a leap in terms of miniaturization of reconfigurable spectral imaging devices by exploring imaging sensors with tunable spectral sensitivities. There are primarily two types of tunable sensors in the literature: sensors whose sensitivities can be tuned in the imaging sensor level, and sensors which have tunable color filter arrays.

Recently, researchers from Politecnico di Milano in Italy proposed a new type of imaging sensor whose sensitivities can be tuned by changing the sensitivities of the sensors themselves [6-8]. This new type of imaging sensor is called Transverse Field Detector (TFD). The TFD takes advantage of the light absorption properties of Silicon. A key optical property of Silicon is that it absorbs different wavelengths of light depending at different depths. Thus, the lower parts of the sensor will absorb longer wavelengths compared to the upper parts of the sensor. By connecting surface electrodes, which produce transverse electric fields throughout the substrate that take advantage of the drift property of electrons, each electrode will then attract electrons coming from different depths in the Silicon. Since electrons coming from different depths in the Silicon are excited by different wavelengths of light, the electrodes can effectively capture the response from different wavelengths of light. By tuning these electrodes, which modify the drift properties of electrons, different absorption spectrums can be obtained. It has been shown that such a sensor could be effective not only for white balance adjustment [9] but also for reconfiguring an imaging sensor for illumination level [10].

A second type of tunable sensor takes the form of tunable color filter arrays as described in [11]. Instead of tuning the sensitivities of the imaging sensor, the absorption spectrum of color filters are modulated instead. Though each pixel element can only record one channel, as in a classical imaging sensor, the spectral sensitivities for each one of these elements can be adjusted, as in the TFD. Since the TFD offers more advantages, we will be discussing using a theoretical device similar to the TFD (in the fact that every pixel has multiple channel read-outs) for the remainder of this study.

Another related work is by Sajadi et. al [12], who proposed an image capture apparatus using switchable primaries by employing shiftable layers of color filter arrays. While this system cannot be tuned pixel-by-pixel, it is a type of adaptive imaging system, which modifies its sensor characteristics based on the scene.

Efficient adaptive spectral imaging

In [13], Langfelder et al. showed that by using the same TFD imaging sensor but by utilizing a non-symmetric electric biasing on the TFD, at a cost of a reduced fill factor due to extra read-out circuitry, it is possible to increase the number of captured channel

from 3 to 5. By redesigning the device it is possible to obtain even more channels by increasing the size of the pixel. This new functionality of the TFD eliminates the necessity of a color filter array and therefore reduces the overall complexity of the system.

By using a tunable spectral imaging sensor, it is possible to build a reconfigurable spectral imaging system that adapts to the content of the scene, increasing capture efficiency. Specific spectral bands are more appropriate for certain reflectances of the scene. For example, if a region of the scene is predominantly red, then it is more appropriate to have pixel sensitivities absorb more red light. Thus, depending on the reflectance of the scene in various regions, the sensor can be tuned to be optimized for the specific reflectance in those regions.

This work performs preliminary simulations of a theoretical imaging system that has spatially tuning spectral sensitivity, where the tuning is based on adaptation to the color content of the capturing scene by performing image analysis of a captured preview. We performed experiments on simulations of tunable sensors versus conventional sensors for multispectral imaging and compared S-CIELAB distances, spectral root mean square (RMS) error as well as metamerism indices for a range of most commonly used illuminants.

Moreover, due to the nature of such tunable imaging sensor, each pixel site can capture data for multiple color channels, eliminating the need for demosaicing on the final image, allowing for higher resolution multispectral images to be captured. The final result is a tunable sensor system which allows for improved performance over traditional multispectral imaging systems

Spectral estimation method

Spectral estimation consists of an inverse problem estimating the full reflectance of the scene at every single position, given input from multiple channels per pixel. Numerous spectral reflectance techniques exist. The most representative methods are outlined in [14]. A few popular spectral estimation methods include the pseudo-inverse method, eigenvector analysis with least squares, and modified-discrete sine transformation. The spectral estimation method used for this study will focus on using the pseudo-inverse method, which produces a linear transformation from the input channels, to the full spectrum of light, by applying the pseudo-inverse operator.

Preview Image Analysis and Filter Tuning

Different pixel sensitivities are optimal for different radiances. For example, when the radiance is predominantly red, it is more useful to have more sensitivity curves capture the longer wavelengths, since most of the information is there. Sampling this curve more finely in the areas that contain more information will result in improved reflectance reconstruction.

In practice tunable sensors such as the TFD cannot be arbitrarily tuned due to device constraints. Therefore, instead of simulating a completely tunable system we adopt an approach that considers a finite collection of sets of spectral sensitivities. Each set of spectral sensitivities will be referred to as a **filter mode**. Thus, the set of spectral sensitivities that are biased toward red regions of the scene would be an example of a filter mode.

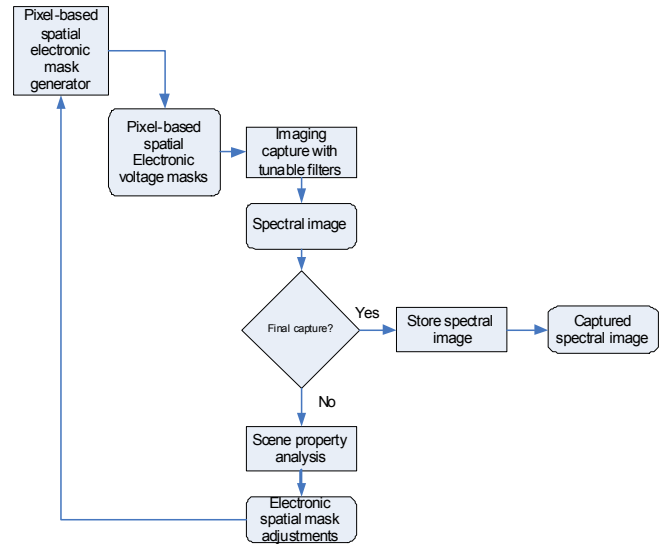


Figure 1: Data flow for the method used in the simulations.

One possible way to bias spectral sensitivities is by applying weights that shifts the sensitivities either towards short or long wavelengths. We adopted seven different filter modes in this study since we empirically found out that seven filter modes would cover most relevant colors. Default mode corresponds to sensitivities that may be found typically in existing multispectral cameras today by equally sampling the visible spectrum, which show no bias towards specific wavelengths. Red mode corresponds to sensitivities that are more densely sampled in longer wavelengths. Blue mode corresponds to sensitivities that are more densely sampled in shorter wavelengths. Figure 1 is a flow diagram for explaining a method of image capture of a scene in which spectral selectivity is adjusted on a region-by-region basis, for imaging sensors with tunable spectral properties, so as to increase spectral differentiation for spectral content in the scene. A default capture parameter (spatial electronic mask) is applied to an imaging assembly having a spectral response which is tunable in accordance with the capture parameter. The spatial electronic mask determines the spectral sensitivities of the sensor for each region. The initial electronic mask could be dictated by the default filter mode. A preview image of a scene is captured and the sample image is analyzed. The optimal filter mode to use is determined based on the scene, on a region-by-region basis. See Figure 2 for an illustration of different filter modes. Additional filter modes are similarly biased towards different areas of the spectrum.

From this information, a spectral mask is constructed for each filter mode. The spectral masks are applied as capture parameters to the imaging assembly by adjusting biasing voltages to each pixel location. These biasing voltages could be determined by look-up-table. Finally, a spectral image of the scene is captured and stored according to the tuned settings.

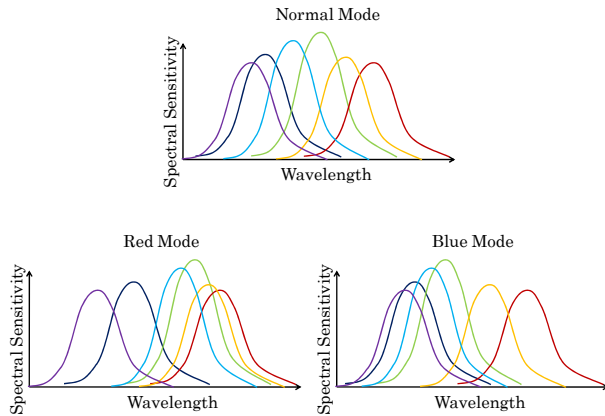


Figure 2: Illustrations of different filter mode spectrums. Notice that the red mode sensitivities have more weight in longer wavelengths while the blue mode sensitivities have more weight near the shorter wavelengths (relative to the default mode).

SVM Filter Mode Selection

The challenge of filter mode selection is anticipating which filter mode is optimal, given an initial preview of the image. There are many possible ways to anticipate the optimal filter mode. A simple way is to simply take the derivative of the channel read-outs from the different sensor channels. The derivative is used since we wish to concentrate the sensitivity curves near sharp drop-offs in the radiance. After the derivative is taken, the position of maximum transition is recorded; this maximum position can then determine which filter mode to use.

Although the previously mentioned method is simple and intuitive, in practice it is difficult to train and utilize, especially on larger amounts of filter modes. The following method is proposed instead: use the derivative of the channel read-outs as features. Taking the derivative of the read-outs allows for invariance to illumination amounts. Next, feed these features into a linear, 1-vs-all support vector machine (SVM). Since the training data has access to the ground truth reflectance, we can determine which filter mode is the most suitable, and use this for training of the SVM.

Experimental Setup

Tunable Sensors

Theoretical tunable sensors, with different modes of operation were used in the experiment. The filters are allowed to switch between filter modes depending on an initial evaluation of the scene. 7 filter modes were used for this experiment, each concentrating in different sections of the visible color spectrum. For this study, only position shifts of filter spectra were considered for constructing filter modes.

Simulation

All simulations were performed using the ISET (Image Systems Evaluation Tools) Toolbox [15]. This toolbox works in conjunction with Matlab® to simulate the complete camera system. White photon noise is included in the simulation to

emulate a real-world scenario. Other real-world factors such as sensor pixel saturation and quantization noise are also modeled by ISET. Complete scenes with known reflectances are used as inputs for the ISET simulation system, which then simulates a lens, and sensor for specific camera systems. We are able to modify the spectral sensitivities for the sensor in order to perform multispectral imaging simulation.

Filter Modes

Seven filter modes are used in the experiment. The filter modes are specialized for the following colors: red, green, blue, yellow, “long-red”, and “short-blue”. Moreover, a default filter mode is left in place for all other cases. The 1-vs-all SVM for filter mode selection was performed using the liblinear 1.8 library, under default settings [16].

Data

16 different scenes with known reflectances were used for this study. The range of ground truth data given was from 400 to 680 nm, in intervals of 10 nm. These multispectral scenes were obtained via different sources. 12 of scenes were from the ISET simulation toolbox, while 6 of the scenes were obtained from a database by Nascimento and Foster [17, 18]. We used 8 random scenes in order to train the linear transformation matrix, and tested the performance of our system on the remaining 8 scenes. See Figure 3 for renderings of this data under original illumination. In order to allow for even sampling of training and testing scenes, the scenes were originally split into 3 sub-databases, scenes with people, scenes with fruits/vegetables, and scenes of foliage. These three sub-databases were then sampled separately in order to obtain the training and testing scenes for the experiment.



Figure 3: sRGB renderings of sample multispectral scenes used for this experiment

In order to produce a more standard comparison, we also evaluated the systems on the GretagMacbeth Color Checker (MCC). Pixels at patch boundaries were masked out in order to obtain color accuracy results only.

Comparisons

The first system we studied was the ISET simulation of a system with a sensor based off of the conventional spectral sensitivities of a multispectral camera. Our pseudo-inverse procedure was used to recover spectral reflectances from the six input channels. In the conventional system, the same filters are applied globally to the whole image. In other words, six separate captures are assumed, with no demosaicing required.

The second system is once again a conventional spectral imaging system. The sensor is simulated with a 6-channel multispectral filter array, and demosaiced with a generic 6-channel demosaicing algorithm as described in [19]. The filters used are identical to the ones used in the first system. In contrast to the first system, the second system only requires one capture, but sacrifices some spatial resolution in exchange. For example, the 50-megapixel multispectral camera exhibited at the 2010 Canon Expo uses a mosaiced multiband acquisition system with 6-channels.

The third system is the new tunable sensor multispectral capture system. As described earlier, this system uses multiple filter modes. The system adaptively chooses between these modes depending on an initial estimation of the spectrum for each pixel in the scene using a linear SVM. See the previous section on filter mode prediction for more details.

Evaluation

We computed the root-mean-square (RMS) spectral error between the conventional and tunable sensor methods and the ground truth reflectances. The RMS conveys the correlation between original and estimated spectral curves.

Moreover, the methods were also evaluated on Euclidean distance in S-CIELAB space [20] averaged among 15 standard illuminants (CIE illuminants A, D50, D65 and F1 to F12) and used 2 degree CIE standard observer in the calculations. In other words, we used 15 standard illuminants for error evaluation and calculated the S-CIELAB (2 degree observer) space distance, when the ground truth reflectance and the estimated reflectance were illuminated with *all* illuminants mentioned above. This distance was then averaged. S-CIELAB metric was used instead of a more traditional metric such as CIEDE2000 because S-CIELAB considers the spatial blurring of the human visual system at different color channels. This type of spatial blurring must be accounted for since we are dealing with real-world images, rather than single colors. Thus, S-CIELAB distance offers a metric that is closer to human perceived error when viewing images, than more conventional metric such as CIEDE2000.

Mean metamerism index (MI) was calculated using the parametric correction proposed by Fairman [21], using CIEDE2000 under 2 degree observer. The metamerism index was measured between the ground truth reflectance, and the estimated reflectance for *all combination* of 15 different illuminants (the same illuminants used for S-CIELAB calculations). These measurements were then averaged for our final metric. The metamerism index conveys the robustness of the spectral

estimation to changes in illumination compared to the original spectra expressed in terms of color difference.

Results and Discussions

Calibration

As discussed previously, calibration was performed separately for each filter mode. For simplicity, the entire training set was used to produce a calibration matrix via the pseudo-inverse method. See Figure 4 for a surface plot of an example calibration matrix. This calibration matrix shows diagonal correlation, exhibiting expected characteristics.

Filter Mode Selection

As expected, the filter modes successfully divide the scene into different regions, depending on dominant transition location. The number of filter modes used is very important. As shown in Figure 5, using as little as 2 filter modes will most likely be sufficient for the tunable sensor spectral imaging system. For our particular simulation, filter modes were hand-picked and it is likely that many of the filter modes are non-optimal. Thus, efforts must be made to develop or adopt techniques to optimize filter modes in the future.

Overall Experiment

We were able to achieve an improvement in performance using tunable sensors versus performance obtained using traditional sensors for multispectral imaging. See Table 1 and Figure 6 a and b for a summary of the comparison.

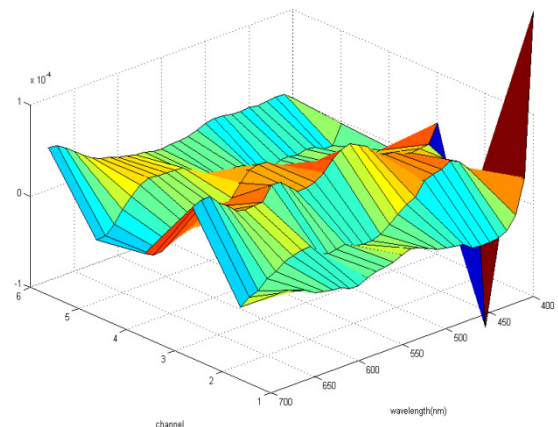


Figure 4: Surface plot for example calibration matrix.

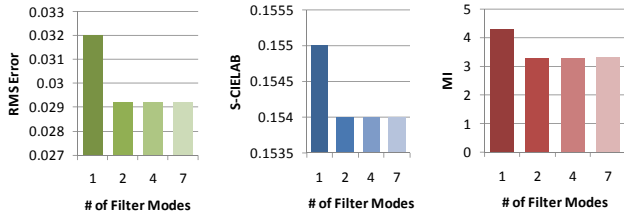


Figure 5: Influence of number of filter modes on performance.

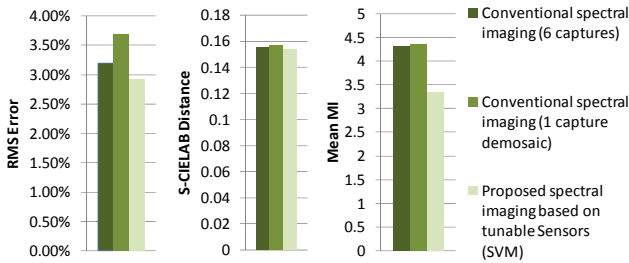


Figure 6a: Average RMS error, S-CIELAB distance, and MI for the entire test set.

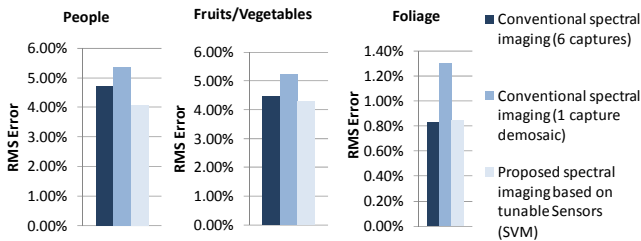


Figure 6b: Average RMS error divided into test set categories. The People category shows the most improvements versus conventional 6 capture imaging, while the Foliage category shows the best performance overall.

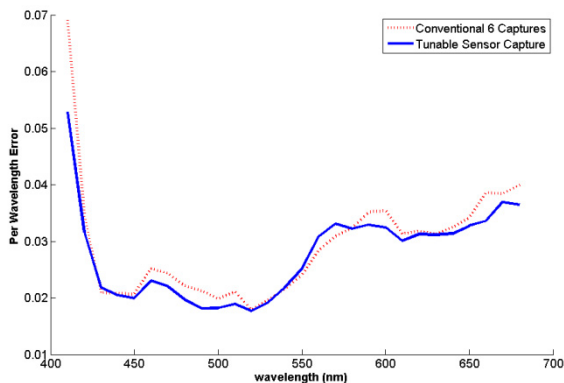


Figure 7: Per wavelength spectral error between ground truth reflectance and both tunable sensor capture and conventional 6 capture systems. As illustrated, tunable sensors can with one capture match and even improve slightly the performance of conventional multi-band capture with 6 channels.

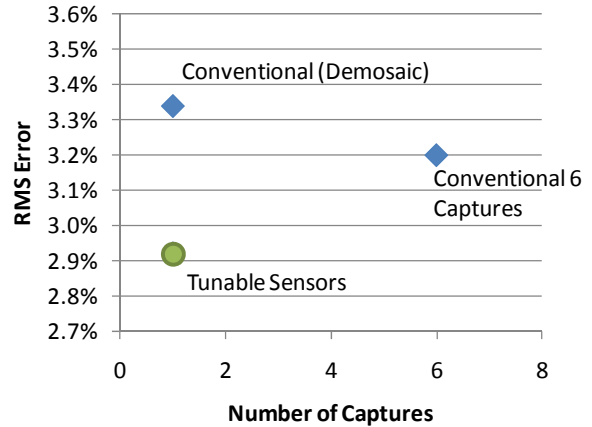


Figure 8: Average RMS Error for spectral imaging using tunable sensors improves over the conventional 6-capture technique, even with only 1 capture.

	RMS Error	S-CIELAB Distance	Mean MI
Conventional multi-capture 6-channel spectral imaging	3.20%	.155	4.32
Conventional single capture 6-channel spectral imaging (Demosaicing required)	3.69%	.157	4.34
Proposed 6-channel spectral imaging based on tunable Sensors (SVM)	2.92%	.154	3.33

Table 1. Summary of experimental results on natural scenes. The tunable sensor configuration shows an improvement of performance over the conventional sensor approach.

Since tunable sensors adapt to the spectral band with more content, they can more efficiently distribute the sensitivity curves to account for the data, and therefore produce more accurate estimated reflectances. These results indicate that tunable sensors show great potential in improving the performance for multispectral cameras, by tuning sensor sensitivities to adapt to the content of the scene prior to image capture.

The adaptability of tunable sensors also results in a much more consistent reproduction of reflectance. Figure 7 depicts spectral error, as calculated on a wavelength-by-wavelength basis. To calculate this spectral error, the RMS error is calculated for each wavelength separately. It is possible to see that the tunable sensor method with one capture outperforms conventional multi-band capture with 6 channels for most of the visible spectrum. The larger errors in the short wavelengths are due to the lack of information in this part of the spectrum due to the combination of low spectral sensitivity of the sensor and low spectral power distribution of halogen illumination used in the captures of several images used in the experiments.

The average performance of the methods was comparable in terms of S-CIELAB distance. In terms of RMS error, the proposed method was able to outperform conventional 6-band capture performance by 9% and the conventional demosaiced 6-channel capture by 21%. As illustrated in Figure 8 the proposed method was able to outperform conventional methods using just one capture. The most noticeable improvement of tunable filter method is shown by the average metamerism index outperforming both conventional multi-capture 6-channel and conventional single capture demosaiced 6-channel methods by approximately 23%. As shown in Figure 6b, the tunable sensor system shows greatest performance gains in the *People* scene category, while all three systems perform the best for the *Foliage* scene category.

As illustrated in Figure 9, the improvements in mean MI come primarily from combinations involving very jagged narrowband fluorescent illuminants (F10 – F12), usually the most difficult illuminants for color reproduction. See Figure 10 for reflectance estimates when the same system (trained on images), was evaluated on the MCC. Estimated reflectance curves for both the conventional capture with 6 bands and tunable sensor methods show reasonable performances, even when trained on real-world images.

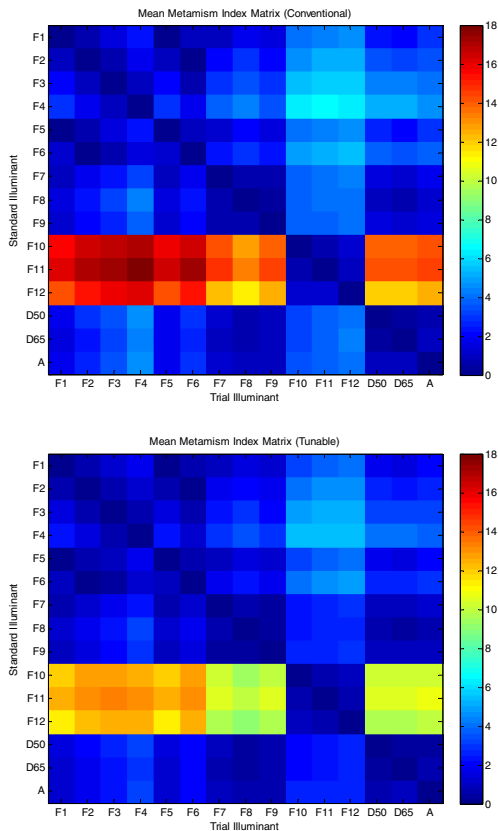


Figure 9: Mean metamerism index matrix visualization for the conventional time multiplexing 6-band imaging (top) and the proposed adaptive tunable sensor imaging (bottom). The color differences were calculated in CIEDE2000 using 2 degree observer. The colors signify the metamerism index for a specific combination of standard and trial illuminants. Notice the large errors amongst the narrowband fluorescent illuminants. The tunable sensor system exhibits large improvements in combinations involving these challenging fluorescent illuminants.

The most important advantage of tunable sensors is perhaps not illustrated by this experiment. The traditional approach for spectral imaging uses multiple image captures, instead of just one (ignoring the preview). Although this multi-shot approach will yield good results for stationary scenes, such scenes in the real-world are rare. Moreover, multi-shot approaches either require a tripod, or an image registration technique. The former is cumbersome, and the latter can degrade image quality. **Although these tunable sensors may provide significant performance benefits, an over-arching advantage may be the convenience and efficiency obtained by using tunable sensors such as the TFD.**

There are some other multi-spectral cameras feature 6 channels in a color filter array (CFA). This camera must be calibrated for specific scenes and reflectances. It is obvious that the tunable sensor configuration will provide better resolution than a multispectral camera based a CFA. In the tunable imaging sensor method all 6 channels are available in each pixel and demosaicing is unnecessary, saving some computation.

An issue not directly addressed in our experiment is the fact that current tunable sensor technology is still relatively limited. For our experiment, we assumed theoretical configurations for sensitivity curves. However, in the real world, tunable sensors such as the TFD have some limitations in adjustable range. Moreover, in order to implement such a system as described above it is required to have a model to convert desirable spectral curves into voltages applied to the tunable imaging sensor and the technology of current devices are not mature enough to allow for a fast adjustment requiring look-up-tables. The hope is that tunable sensor technology will advance fast enough to allow for such adjustments in the very near future.

While our results are promising, there are additional experiments to be performed to further show the benefit of tunable sensors over traditional sensors for multispectral imaging. For example, our current set of data is still limited, and we would like to run more simulations with more datasets in the future. Moreover, while our filter mode selection mechanism works reasonably well, other approaches for filter mode selection may be superior or more efficient. Currently, the filter modes are picked manually and do not consider width or height modulation of the curves. More optimal filter mode selection could potentially boost performance quite a bit but we need to consider implementability issues as well.

More realistic simulation details should also be considered. Although the current simulation includes white photon noise, real-world sensor noise, which could potentially be extremely important, has not been included in this simulation. Currently, spectral sensitivity curves may be shifted arbitrarily, and their shape is completely flexible; future simulations must take into account physical spectral sensitivity constraints of the tunable sensor.

Conclusion

Tunable sensors such as the TFD can bring potential improvements to the imaging industry. One such application is in multi-spectral imaging, where the sensors can be tuned differently depending on estimated reflectance of the scene. This study performed preliminary simulations of a tunable sensor system using ISET, which provides a reliable simulation environment. As

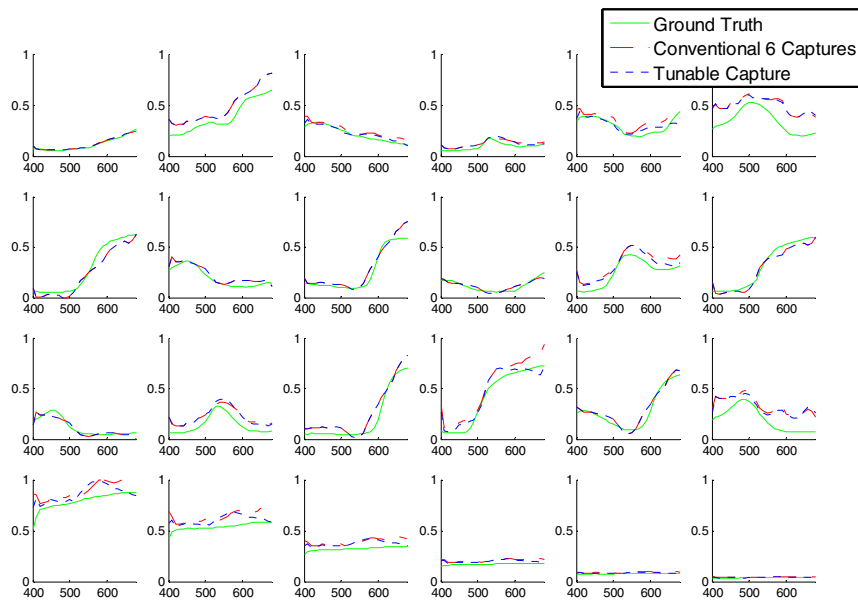


Figure 10: Reflectance plots for the GretagMacbeth Color Checker (MCC). Plots are in the same configuration as patches on the color checker. In each plot, the x-axis denotes wavelength in nm, and y-axis denotes percentage reflectance.

a result, it was possible to obtain improvement in efficiency over conventional multi-band imaging sensor systems in terms of metamerism index and RMS. The spectral imaging method based on tunable imaging sensor presents not just superior spectral estimation performance, but dramatically increases the efficiency and convenience of multispectral imaging compared to traditional multispectral cameras. This study points out to a new paradigm in reconfigurable spectral imaging by adapting to the scene and computationally reconfiguring the imaging capture based on calibration performed using images decreasing the current dependency of spectral imaging system on calibration targets.

References

- [1] S. Tominaga, Spectral imaging by a multichannel camera, *J. Electron. Imaging* **8**, 332-341 (1999).
- [2] G. Shaw and H. Burke, "Spectral imaging for remote sensing," *Lincoln Laboratory Journal* **14**, 3–28, (2003).
- [3] R. S. Berns, Color-accurate image archives using spectral imaging, Scientific examination of art: modern techniques in conservation and analysis, National Academies Press, pp. 105-119 (2005).
- [4] A. Mohan, R. Raskar and J. Tumblin, Agile Spectrum Imaging: Programmable wavelength modulation for cameras and projectors, *Computer Graphics Forum* **27**, 709-717 (2008).
- [5] M. Hauta-Kasari, K. Miyazawa, S. Toyooka and J. Parkkinen, Spectral Vision System for Measuring Color Images, *J. Opt. Soc. Am. A* **16**, 2352-2362 (1999).
- [6] A. Longoni, F. Zaraga, G. Langfelder and L. Bombelli, "The Transverse Field Detector (TFD): A Novel Color-Sensitive CMOS Device," *IEEE Electron Device Lett.* **29**, 1306-1308, (2008).
- [7] G. Langfelder, F. Zaraga, and A. Longoni. "Tunable Spectral Responses in a Color-Sensitive CMOS Pixel for Imaging Applications," *IEEE Trans. Electron Devices* **56**, 2563-2569 (2009).
- [8] G. Langfelder, "Design of a fully CMOS compatible 3- μm size color pixel," *Microelectron. Reliab.* **50**, 163-173 (2010).
- [9] F. Zaraga and G. Langfelder, White balance by tunable spectral responsivities, *J. Opt. Soc. Am. A* **27**, 31-39 (2010).
- [10] F. Zaraga, G. Langfelder and A. Longoni, Implementation of an Interleaved Image sensor by means of the filterless Transverse Field Detector (TFD), *J. Electron. Imaging* **19**, 033013 (2010).
- [11] D. Miller, "Methods for adaptive spectral, spatial and temporal sensing for imaging applications," U.S. Patent 6466961, Oct. 15, 2002.
- [12] B. Sajadi, A. Majumder, K. Hiwada, A. Maki and R. Raskar. Switchable Primaries Using Shiftable Layers of Color Filter Arrays. *ACM Trans. Graph.* **30**, 4, Article 65 (2011).
- [13] G. Langfelder, A.F. Longoni and F. Zaraga, Implementation of a multi-spectral color imaging device without color filter array, *Proc. SPIE 7876, Digital Photography VII*, 2011, 787608.
- [14] F. Imai, L. Taplin and E. Day, "Comparison of the accuracy of various transformations from multi-band images to reflectance spectra," *Munsell Color Science Laboratory Technical Report*, 2002. http://art-si.org/PDFs/Art-SI_Summer2002.pdf
- [15] J. E. Farrell, F. Xiao, P. Cattrysse and B. Wandell, A simulation tool for evaluating digital camera image quality, A simulation tool for evaluating digital camera image quality, *Proc. SPIE 5294*, 2004, pp. 124-131.
- [16] R.-E. Fan, K.-W. Chang, C.-J. Hsieh, X.-R. Wang and C.-J. Lin. LIBLINEAR: A library for large linear classification *Journal of Machine Learning Research* **9**, 1871-1874 (2008).
- [17] S. M. C. Nascimento, F. Ferreira and D. H. Foster, Statistics of spatial cone-excitation ratios in natural scenes. *Journal of the Optical Society of America A* **19**, 1484-1490 (2002).
- [18] D. H. Foster, S.M.C Nascimento and K. Amano, Information limits on neural identification of coloured surfaces in natural scenes, *Visual Neuroscience* **21**, 331-336 (2004).
- [19] L. Miao, H. Qi, R. Ramanath and W. Snyder, Binary Tree-based Generic Demosaicking Algorithm for Multispectral Filter Arrays. *IEEE Transaction on Image Processing* **15**, 3350-3558 (2006).
- [20] X. Zhang and B. Wandell, A spatial extension of CIELAB for digital color reproduction, *Proc. Soc. oc. Inform. Display 96 Digest*, 1996, pp. 731-734.
- [21] H. Fairman, Metameric Correction Using Parameric Decomposition. *Color Research & Application* **12**, 261-265 (1987).